Deeply bound T_{bb} and near-threshold BB^* scattering with a relativistic heavy quark action

Andres Stump
Jeremy R. Green

Lattice Conference 2026, University of Maryland
July 30, 2026

Humboldt-Universität zu Berlin

T_{bb} tetraquark and BB^* scattering

- Bottom analog of T_{cc}: $\overline{b}\overline{b}ud$, $I(J^P) = 0(1^+)$
  $\rightarrow$ appears in the BB^* system

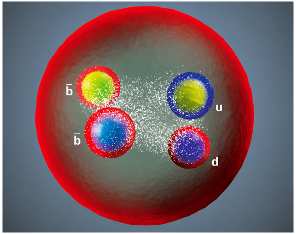

T_{bb} tetraquark and BB^* scattering

- Bottom analog of T_{cc}: $\overline{bb}ud$, $I(J^P) = 0(1^+)$
  $\rightarrow$ appears in the BB^* system
- Not (yet) seen in experiment

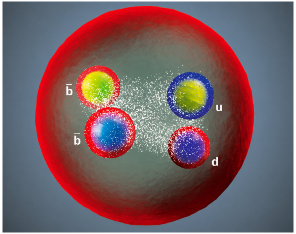

T_{bb} tetraquark and BB^* scattering

- Bottom analog of T_{cc}: $\overline{b}\overline{b}ud$, $I(J^P) = 0(1^+)$
  $\rightarrow$ appears in the BB^* system
- Not (yet) seen in experiment
- Broad consensus: **deeply bound**
  [Leskovec et al. 2019; Alexandrou et al. 2024; Hoffmann and Meinel 2026]

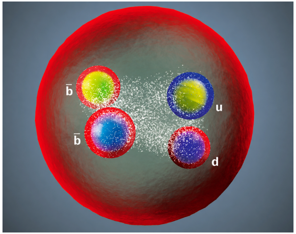

T_{bb} tetraquark and BB^* scattering

- Bottom analog of T_{cc}: $\overline{b}\overline{b}ud$, $I(J^P) = 0(1^+)$
  $\rightarrow$ appears in the BB^* system
- Not (yet) seen in experiment
- Broad consensus: **deeply bound**
  [Leskovec et al. 2019; Alexandrou et al. 2024; Hoffmann and Meinel 2026]
- Almost nothing known about BB^* scattering close to/above threshold

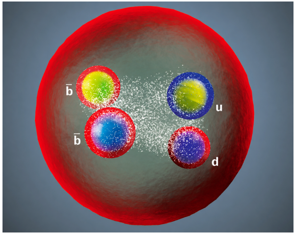

T_{bb} tetraquark and BB^* scattering

- Bottom analog of T_{cc}: $\overline{b}\overline{b}ud$, $I(J^P) = 0(1^+)$
  $\rightarrow$ appears in the BB^* system
- Not (yet) seen in experiment
- Broad consensus: **deeply bound**
  [Leskovec et al. 2019; Alexandrou et al. 2024; Hoffmann and Meinel 2026]
- Almost nothing known about BB^* scattering close to/above threshold

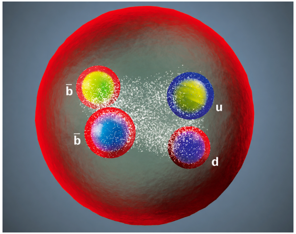

$\rightarrow$ **Goal:** Investigate T_{bb} binding energy *and* BB^* scattering

Why the BB^* system is hard

- Large $B^{(*)}$ masses
  - $\rightarrow$ Dense finite-volume spectrum

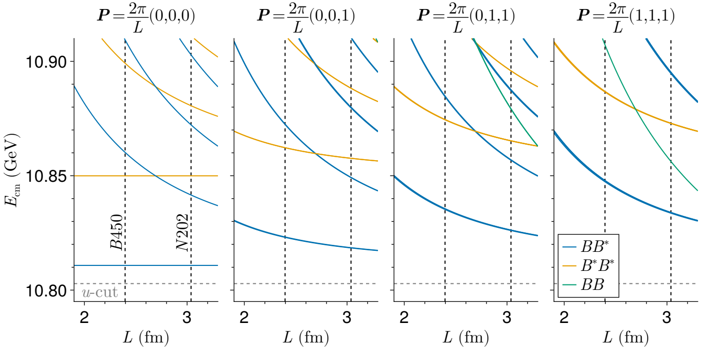

Figure: Noninteracting $B^{(*)}B^*$ c.m. levels

Why the BB^* system is hard

- Large $B^{(*)}$ masses
  $\rightarrow$ Dense finite-volume spectrum
- Large operator basis needed:
  - **Local** tetraquark operators:
    Essential for T_{bb}
  - **Bilocal** two-meson operators:
    For the BB^* scattering

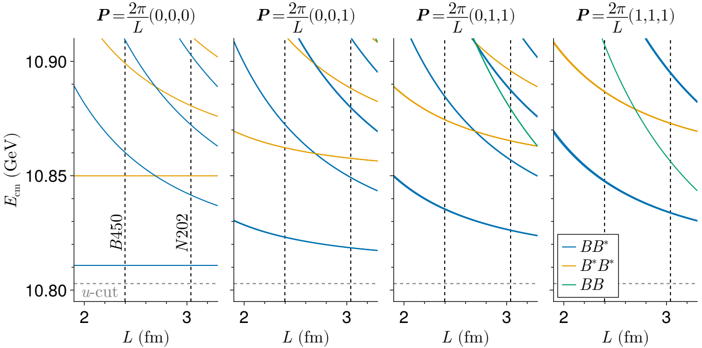

Figure: Noninteracting $B^{(*)}B^*$ c.m. levels

Why the BB^* system is hard

- Large $B^{(*)}$ masses
  $\rightarrow$ Dense finite-volume spectrum
- Large operator basis needed:
  - **Local** tetraquark operators: Essential for T_{bb}
  - **Bilocal** two-meson operators: For the BB^* scattering
- Small B–B^* splitting (≈ 40 MeV)
  - Low B^*B^* threshold
  - Limits range of validity of single-channel Lüscher formalism

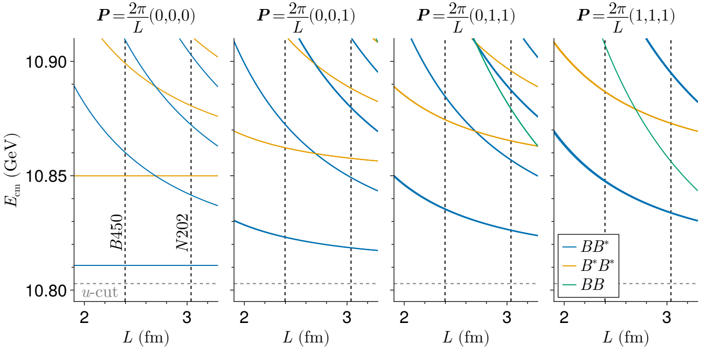

Figure: Noninteracting $B^{(*)}B^*$ c.m. levels

Content

1. Lattice setup
2. B and B^* mesons
3. Local tetraquark operators in distillation
4. Results for the BB^* system (Exploratory!)
   - T_{bb} binding energy
   - Finite-volume BB^* spectrum
   - Single-channel s-wave Lüscher analysis

Lattice setup

Lattice setup and RHQ action

CLS gauge ensembles (B450, N202):

- $N_f = 3$ Wilson clover fermions
- $SU(3)$-flavour-symmetric point:
  - physical $\frac{1}{3}(m_u + m_d + m_s)$
  - $m_\pi \approx 420$ MeV

Ensemble	$N_s^3 \times N_t$	a [fm]	L [fm]	N_v
B450	$32^3 \times 64$	0.0749	2.4	32
N202	$48^3 \times 128$	0.0633	3.0	68

Lattice setup and RHQ action

CLS gauge ensembles (B450, N202):

- $N_f = 3$ Wilson clover fermions
- $SU(3)$-flavour-symmetric point:
  - physical $\frac{1}{3}(m_u + m_d + m_s)$
  - $m_\pi \approx 420$ MeV

Ensemble	$N_s^3 \times N_t$	a [fm]	L [fm]	N_v
B450	$32^3 \times 64$	0.0749	2.4	32
N202	$48^3 \times 128$	0.0633	3.0	68

Bottom quark:

- Use RHQ action [Aoki, Kuramashi, and Tominaga 2003]: (asymmetry between space and time)
- 5-parameter action
- Tuned nonperturbatively [Hudspith and Mohler 2022]:
  - 5 physical bottomonium masses
  - $c^2 = 1$

B and B^* mesons

Dispersion relation:

- Investigated speed-of-light parameter

$$E_B(\boldsymbol{p})^2 = m_B^2 + c_B^2\,\boldsymbol{p}^2$$

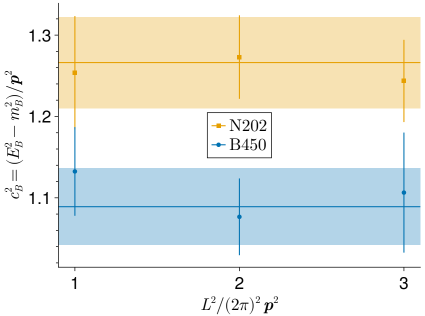

Figure: Speed-of-light parameter for B

Dispersion relation:

- Investigated speed-of-light parameter

$$E_B(\boldsymbol{p})^2 = m_B^2 + c_B^2\,\boldsymbol{p}^2$$

$\rightarrow$ Significantly above one on N202

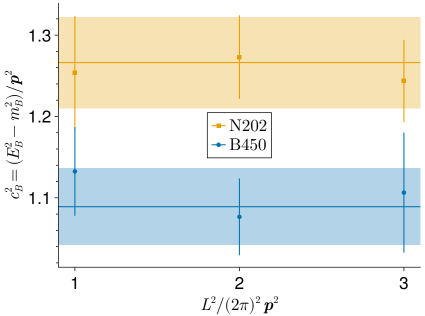

Figure: Speed-of-light parameter for B

Dispersion relation:

- Investigated speed-of-light parameter

$$E_B(\boldsymbol{p})^2 = m_B^2 + c_B^2\,\boldsymbol{p}^2$$

$\rightarrow$ Significantly above one on N202

- Possible reasons:
  - Large excited-state contamination at $\boldsymbol{p} \neq \mathbf{0}$ (e.g. due to the large smearing radius)
  - Mistuning of the RHQ action

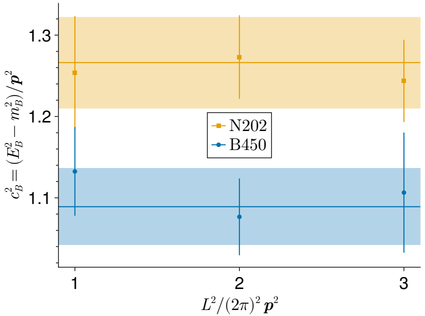

Figure: Speed-of-light parameter for B

Dispersion relation:

- Investigated speed-of-light parameter

$$E_B(\boldsymbol{p})^2 = m_B^2 + c_B^2\,\boldsymbol{p}^2$$

$\rightarrow$ Significantly above one on N202

- Possible reasons:
  - Large excited-state contamination at $\boldsymbol{p} \neq \boldsymbol{0}$ (e.g. due to the large smearing radius)
  - Mistuning of the RHQ action
- Variational analysis with covariant-derivative operators:

$\rightarrow$ Reduces estimates of c_B^2 ($c_B^2 = 1.12(3)$)

$\rightarrow$ Indicates large excited-state contamination

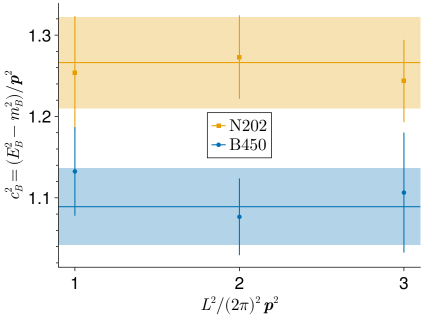

Figure: Speed-of-light parameter for B

B and B^* mesons

Dispersion relation:

- Investigated speed-of-light parameter

$$E_B(\boldsymbol{p})^2 = m_B^2 + c_B^2\, \boldsymbol{p}^2$$

  $\rightarrow$ Significantly above one on N202
- Possible reasons:
  - Large excited-state contamination at $\boldsymbol{p} \neq \boldsymbol{0}$ (e.g. due to the large smearing radius)
  - Mistuning of the RHQ action
- Variational analysis with covariant-derivative operators:
  $\rightarrow$ Reduces estimates of c_B^2 ($c_B^2 = 1.12(3)$)
  $\rightarrow$ Indicates large excited-state contamination

$\rightarrow$ Need to handle excited states *and* correct for the dispersion relation for $B^{(*)}B^*$ states

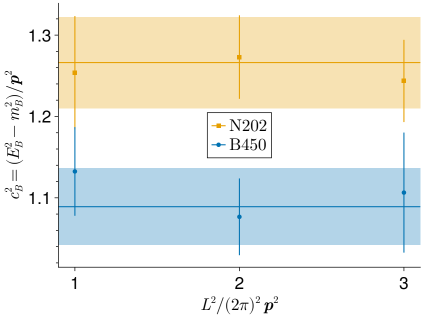

Figure: Speed-of-light parameter for B

B and B^* mesons

Dispersion relation:

- Investigated speed-of-light parameter

$$E_B(\boldsymbol{p})^2 = m_B^2 + c_B^2\, \boldsymbol{p}^2$$

  $\rightarrow$ Significantly above one on N202

- Possible reasons:
  - Large excited-state contamination at $\boldsymbol{p} \neq \boldsymbol{0}$ (e.g. due to the large smearing radius)
  - Mistuning of the RHQ action

- Variational analysis with covariant-derivative operators:

  $\rightarrow$ Reduces estimates of c_B^2 ($c_B^2 = 1.12(3)$)

  $\rightarrow$ Indicates large excited-state contamination

$\rightarrow$ Need to handle excited states *and* correct for the dispersion relation for $B^{(*)}B^*$ states

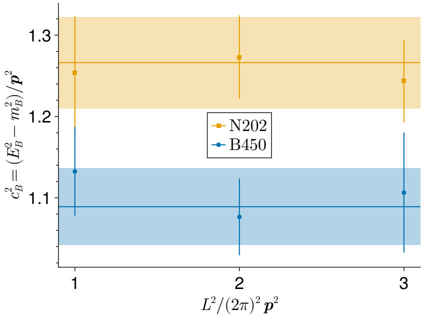

Figure: Speed-of-light parameter for B

Future plans: Repeat calculation with improved $B^{(*)}$ operator

Local tetraquark operators in distillation

Distillation + position-space sampling for local tetraquark operators

Laplacian Heaviside (LapH) smearing:

- Perambulator: $\tau(t', t) = V(t')^\dagger \, S(t', t) \, V(t)$
- $V(t)$ contains N_v lowest eigenvectors of $\Delta(t)$

Distillation + position-space sampling for local tetraquark operators

Laplacian Heaviside (LapH) smearing:

- Perambulator: $\tau(t', t) = V(t')^\dagger\, S(t', t)\, V(t)$
- $V(t)$ contains N_v lowest eigenvectors of $\Delta(t)$

Local tetraquark operators (e.g. diquark-antidiquark):

$$\mathcal{O}^T(t) \sim (\overline{b}\overline{b}ud)(\boldsymbol{P}, t)$$

- N_v^5 cost scaling in "traditional" distillation

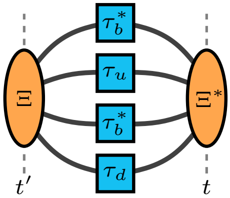

Laplacian Heaviside (LapH) smearing:

- Perambulator: $\tau(t',t) = V(t')^\dagger \, S(t',t) \, V(t)$
- $V(t)$ contains N_v lowest eigenvectors of $\Delta(t)$

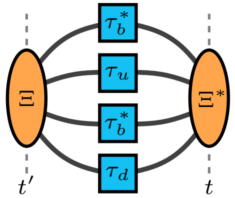

Local tetraquark operators (e.g. diquark-antidiquark):

$$\mathcal{O}^T(t) \sim (\overline{b}\overline{b}ud)(\boldsymbol{P},t)$$

- N_v^5 cost scaling in "traditional" distillation

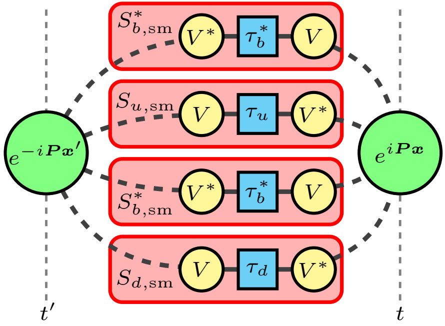

Postion-space sampling method [AS and Green 2026]

- Explicitly compute smeared propagators (N_v^3 cost)

$$S_{f,\,\mathrm{sm}}(t',t) = V(t') \cdot \tau_f(t',t) \cdot V(t)^\dagger$$

- Sum only over regular sparse grids with random offsets

Laplacian Heaviside (LapH) smearing:

- Perambulator: $\tau(t', t) = V(t')^\dagger \, S(t', t) \, V(t)$
- $V(t)$ contains N_v lowest eigenvectors of $\Delta(t)$

Local tetraquark operators (e.g. diquark-antidiquark):

$$\mathcal{O}^T(t) \sim (\overline{b}\overline{b}ud)(\boldsymbol{P}, t)$$

- N_v^5 cost scaling in "traditional" distillation

Postion-space sampling method [AS and Green 2026]

- Explicitly compute smeared propagators (N_v^3 cost)

$$S_{f,\,\mathrm{sm}}(t', t) = V(t') \cdot \tau_f(t', t) \cdot V(t)^\dagger$$

- Sum only over regular sparse grids with random offsets

→ Makes tetraquark operators affordable in distillation!

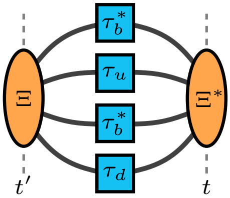

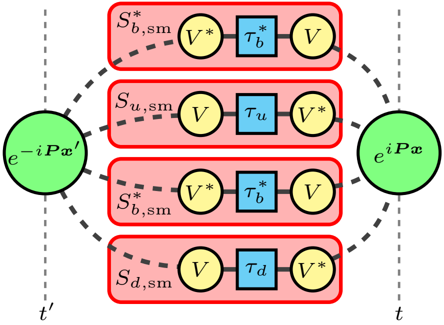

Results for the BB^* system (Exploratory!)

Operator basis

Large operator basis:

- Bilocal two-meson operators (BB^* and B^*B^*)
- Local tetraquark operators (local $B^{(*)}B^*$, BB_0^*, diquark-antidiquark)

$\boldsymbol{D} = \frac{L}{2\pi}\boldsymbol{P}$	$(0,0,0)$	$(0,0,1)$	$(0,1,1)$	$(1,1,1)$
Irrep	T_1^+	A_2	A_2	A_2
# bilocal operators	12	9	6	9
Total # operators	15	13	10	13

- Well below the left-hand cut from one-pion exchange
  $\rightarrow$ cannot apply Lüscher

T_{bb} binding energy

- Well below the left-hand cut from one-pion exchange
  $\rightarrow$ cannot apply Lüscher
- Deeply bound ($\mathrm{e}^{-m_\pi L}$ volume effects)
  $\rightarrow$ T_{bb} is the finite-volume ground state

T_{bb} binding energy

- Well below the left-hand cut from one-pion exchange
  $\rightarrow$ cannot apply Lüscher
- Deeply bound ($e^{-m_\pi L}$ volume effects)
  $\rightarrow$ T_{bb} is the finite-volume ground state
- Difficulty: no clear plateau in the effective energy
  $\rightarrow$ fits at late, noisy times
  - Likely too large LapH smearing radius
  - N202: cross-check with Generalized Pencil of Function method

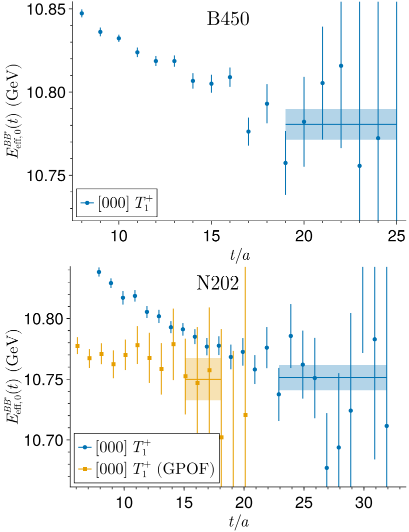

Figure: Ground state E_{eff} of BB^* system

T_{bb} binding energy

- Well below the left-hand cut from one-pion exchange
  $\rightarrow$ cannot apply Lüscher
- Deeply bound ($e^{-m_\pi L}$ volume effects)
  $\rightarrow$ T_{bb} is the finite-volume ground state
- Difficulty: no clear plateau in the effective energy
  $\rightarrow$ fits at late, noisy times
  - Likely too large LapH smearing radius
  - N202: cross-check with Generalized Pencil of Function method

$\rightarrow$ Binding energies are **lower bounds**

$$m_B + m_{B^*} - m_{T_{bb}} = \begin{cases} 53(8)\ \text{MeV} & \text{(B450)}, \\ 61(17)\ \text{MeV} & \text{(N202)} \end{cases}$$

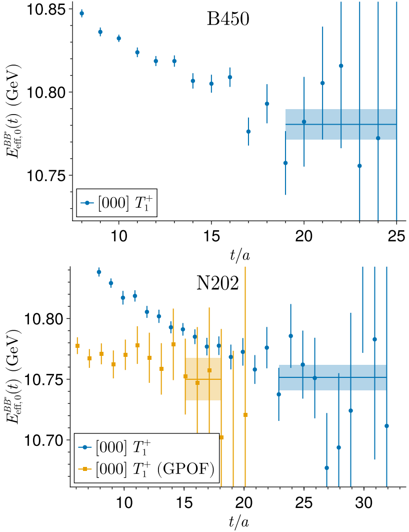

Figure: Ground state E_{eff} of BB^* system

T_{bb} binding energy

- Well below the left-hand cut from one-pion exchange
  $\rightarrow$ cannot apply Lüscher
- Deeply bound ($e^{-m_\pi L}$ volume effects)
  $\rightarrow$ T_{bb} is the finite-volume ground state
- Difficulty: no clear plateau in the effective energy
  $\rightarrow$ fits at late, noisy times
  - Likely too large LapH smearing radius
  - N202: cross-check with Generalized Pencil of Function method

$\rightarrow$ Binding energies are **lower bounds**

$$m_B + m_{B^*} - m_{T_{bb}} = \begin{cases} 53(8)\ \text{MeV} & \text{(B450)}, \\ 61(17)\ \text{MeV} & \text{(N202)} \end{cases}$$

- In agreement with other RHQ results at similar m_π
  [Hoffmann and Meinel 2026; Vujmilovic et al. 2026]

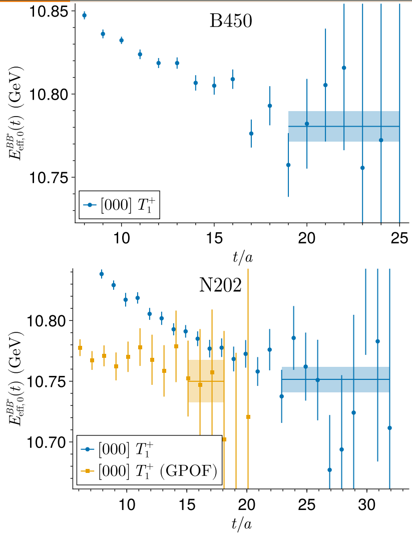

Figure: Ground state E_{eff} of BB^* system

Extracting excited $B^{(*)}B^*$ energies

Extract $\Delta E_n^{B^{(*)}B^*}$ to the nearest noninteracting level
$\rightarrow$ strong (empirical) cancellation of excited-state effects

Extracting excited $B^{(*)}B^*$ energies

Extract $\Delta E_n^{B^{(*)}B^*}$ to the nearest noninteracting level
$\rightarrow$ strong (empirical) cancellation of excited-state effects

Two fitting strategies:

1. Fits to effective energy differences ("ratio" fits)

$$\Delta E_{\text{eff},n}^{B^{(*)}B^*}(t) = E_{\text{eff},n}^{B^{(*)}B^*}(t) - E_{\text{eff}}^{B^{(*)}(\boldsymbol{p}_1)}(t) - E_{\text{eff}}^{B^*(\boldsymbol{p}_2)}(t)$$

- Fit only where all E_{eff} have plateaued (if possible)

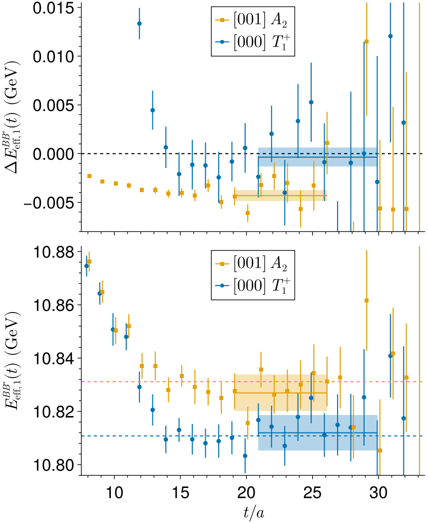

Figure: First excited state on N202: ΔE_{eff} (top) and E_{eff} (bottom)

Extracting excited $B^{(*)}B^*$ energies

Extract $\Delta E_n^{B^{(*)}B^*}$ to the nearest noninteracting level
$\rightarrow$ strong (empirical) cancellation of excited-state effects

Two fitting strategies:

1. Fits to effective energy differences ("ratio" fits)

$$\Delta E_{\text{eff},n}^{B^{(*)}B^*}(t) = E_{\text{eff},n}^{B^{(*)}B^*}(t) - E_{\text{eff}}^{B^{(*)}(\boldsymbol{p}_1)}(t) - E_{\text{eff}}^{B^*(\boldsymbol{p}_2)}(t)$$

   - Fit only where all E_{eff} have plateaued (if possible)

2. Combined fits to the three effective energies

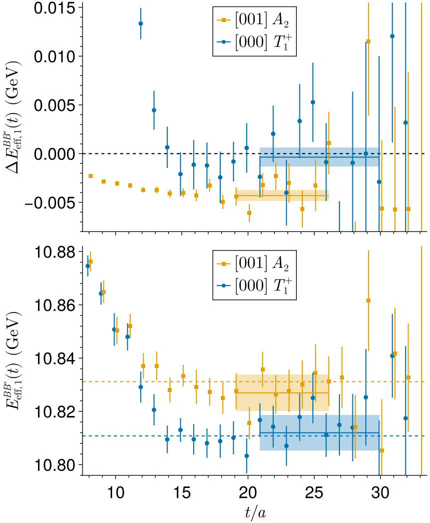

Figure: First excited state on N202: ΔE_{eff} (top) and E_{eff} (bottom)

Extracting excited $B^{(*)}B^*$ energies

Extract $\Delta E_n^{B^{(*)}B^*}$ to the nearest noninteracting level
$\rightarrow$ strong (empirical) cancellation of excited-state effects

Two fitting strategies:

1. Fits to effective energy differences ("ratio" fits)

$$\Delta E_{\mathrm{eff},n}^{B^{(*)}B^*}(t) = E_{\mathrm{eff},n}^{B^{(*)}B^*}(t) - E_{\mathrm{eff}}^{B^{(*)}(\boldsymbol{p}_1)}(t) - E_{\mathrm{eff}}^{B^*(\boldsymbol{p}_2)}(t)$$

   - Fit only where all E_{eff} have plateaued (if possible)

2. Combined fits to the three effective energies

Spread between the strategies $\rightarrow$ systematic error

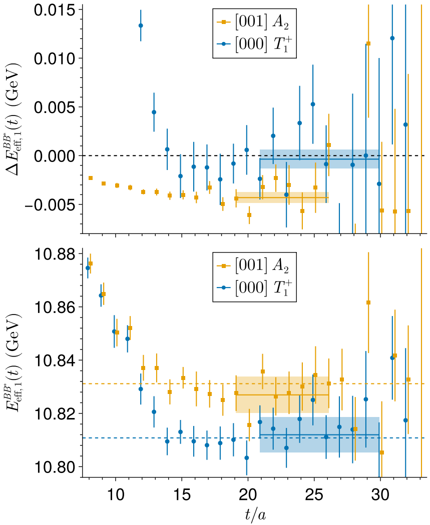

Figure: First excited state on N202: ΔE_{eff} (top) and E_{eff} (bottom)

Extracting excited $B^{(*)}B^*$ energies

Extract $\Delta E_n^{B^{(*)}B^*}$ to the nearest noninteracting level
$\rightarrow$ strong (empirical) cancellation of excited-state effects

Two fitting strategies:

1. Fits to effective energy differences ("ratio" fits)

$$\Delta E_{\mathrm{eff},n}^{B^{(*)}B^*}(t) = E_{\mathrm{eff},n}^{B^{(*)}B^*}(t) - E_{\mathrm{eff}}^{B^{(*)}(\boldsymbol{p}_1)}(t) - E_{\mathrm{eff}}^{B^*(\boldsymbol{p}_2)}(t)$$

   - Fit only where all E_{eff} have plateaued (if possible)

2. Combined fits to the three effective energies

Spread between the strategies $\rightarrow$ systematic error

Dispersion-relation correction:
$\rightarrow$ Use *continuum* noninteracting energies

$$E_n^{B^{(*)}B^*} = \Delta E_n^{B^{(*)}B^*} + \sqrt{m_{B^{(*)}}^2 + \boldsymbol{p}_1^2} + \sqrt{m_{B^*}^2 + \boldsymbol{p}_2^2}$$

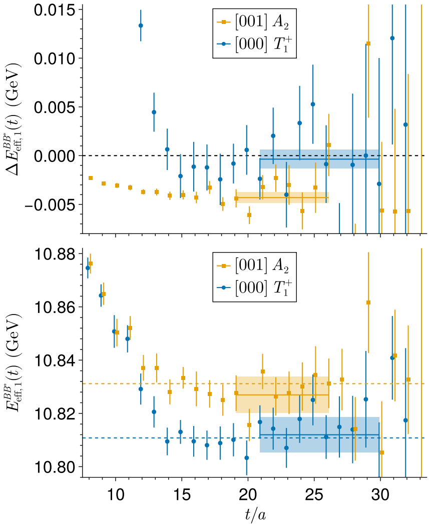

Figure: First excited state on N202: ΔE_{eff} (top) and E_{eff} (bottom)

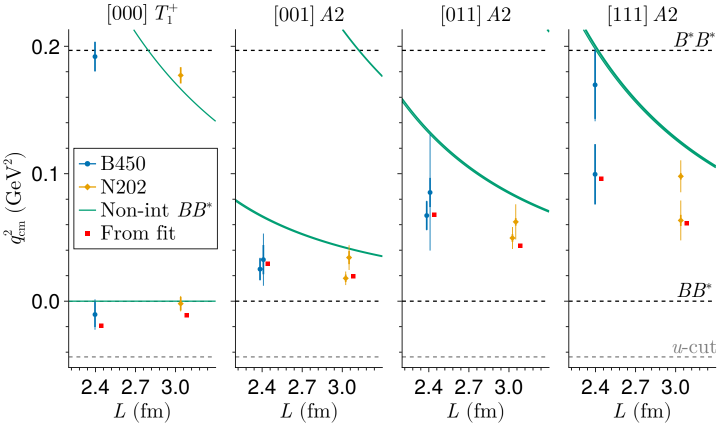

Figure: Excited $B^{(*)}B^*$ states

Finite-volume $B^{(*)}B^*$ spectrum

- Ground state (T_{bb}) below u-cut
  $\rightarrow$ not usable for Lüscher analysis

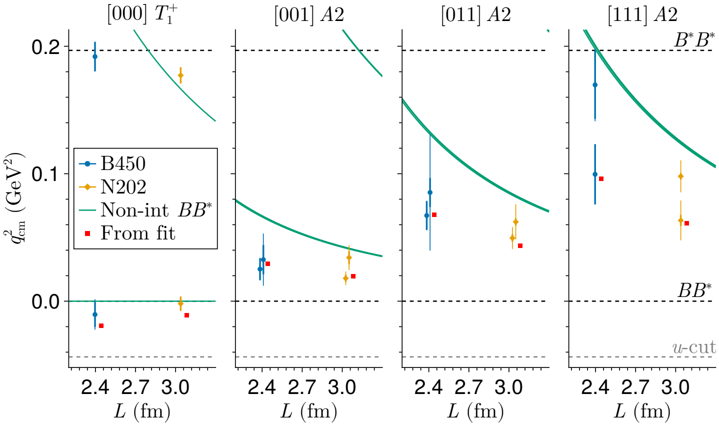

Figure: Excited $B^{(*)}B^*$ states

Finite-volume $B^{(*)}B^*$ spectrum

- Ground state (T_{bb}) below u-cut
  $\rightarrow$ not usable for Lüscher analysis
- Use the **first excited states**
  (well below B^*B^*)

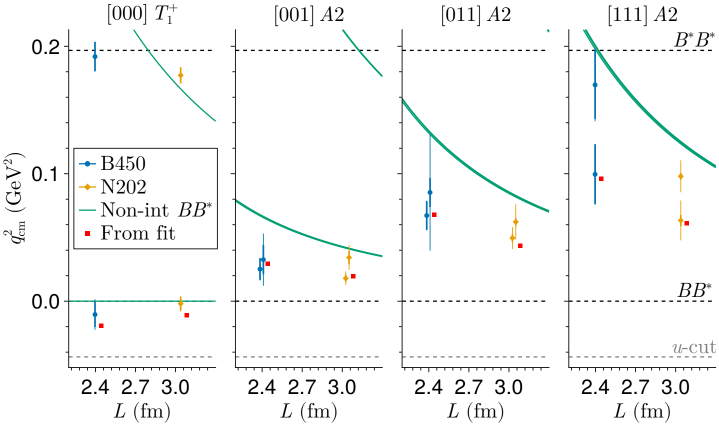

Figure: Excited $B^{(*)}B^*$ states

Single-channel s-wave Lüscher analysis

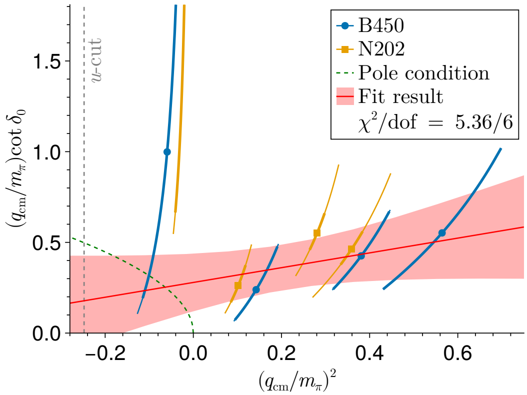

Figure: s-wave BB^* scattering phase shift

Single-channel s-wave Lüscher analysis

- Linear effective range expansion

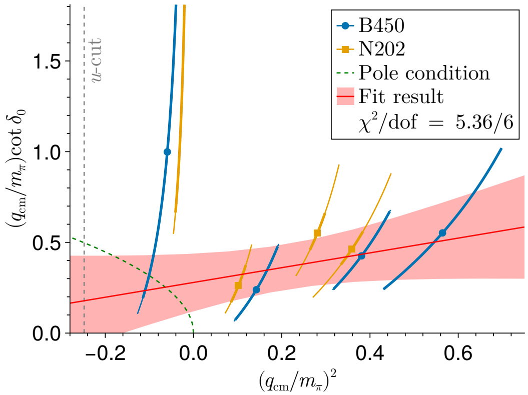

Figure: s-wave BB^* scattering phase shift

BB^* scattering near threshold

Single-channel s-wave Lüscher analysis

- Linear effective range expansion
- Combined fit to both ensembles

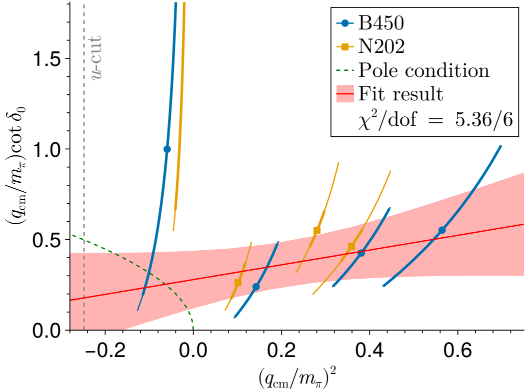

Figure: s-wave BB^* scattering phase shift

Single-channel s-wave Lüscher analysis

- Linear effective range expansion
- Combined fit to both ensembles
- Good fit quality
  $\rightarrow$ Consistent values for phase shift

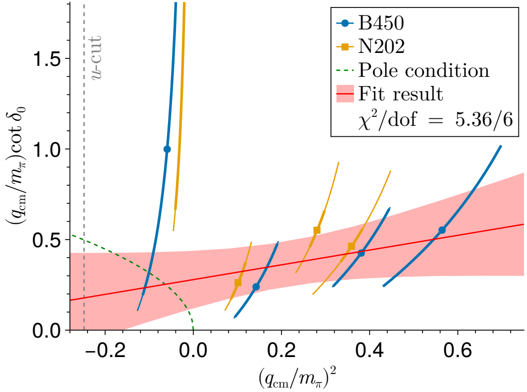

Figure: s-wave BB^* scattering phase shift

BB^* scattering near threshold

Single-channel s-wave Lüscher analysis

- Linear effective range expansion
- Combined fit to both ensembles
- Good fit quality
  $\rightarrow$ Consistent values for phase shift
- Crossing with the pole condition:
  - Strong indication of **shallow virtual bound state**
  - $2(2)_{\mathrm{stat}}(1)_{\mathrm{sys}}$ MeV below threshold
  - Distortion due to one-pion exchange?

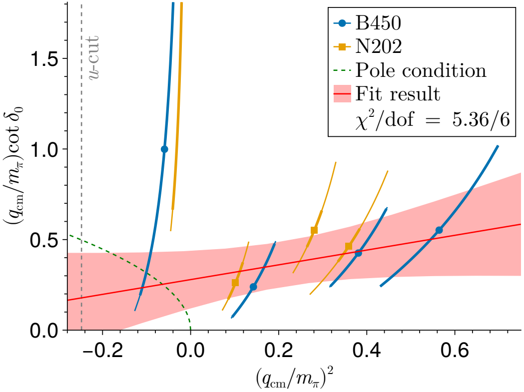

Figure: s-wave BB^* scattering phase shift

BB^* scattering near threshold

Single-channel s-wave Lüscher analysis

- Linear effective range expansion
- Combined fit to both ensembles
- Good fit quality

  $\rightarrow$ Consistent values for phase shift
- Crossing with the pole condition:
  - Strong indication of **shallow virtual bound state**
  - $2(2)_{\mathrm{stat}}(1)_{\mathrm{sys}}$ MeV below threshold
  - Distortion due to one-pion exchange?
- Heavy-quark spin symmetry:
  - A bound BB^* state has a near-degenerate B^*B^* partner
  - Relation to T_{cc} and T'_{cc} in DD^*–D^*D^* system [Whyte, Wilson, and Thomas 2025]

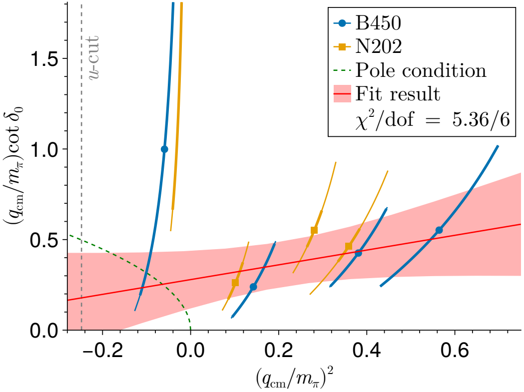

Figure: s-wave BB^* scattering phase shift

Conclusion

- Investigation of BB^* system with RHQ action:
  - $m_\pi \approx 420$ MeV
  - Large basis of local and bilocal operators in distillation

Conclusion

- Investigation of BB^* system with RHQ action:
  - $m_\pi \approx 420$ MeV
  - Large basis of local and bilocal operators in distillation
- Binding energy of the T_{bb}: $\sim 55\,\mathrm{MeV}$ (lower bound)
  $\rightarrow$ Consistent with other RHQ results

Conclusion

- Investigation of BB^* system with RHQ action:
  - $m_\pi \approx 420$ MeV
  - Large basis of local and bilocal operators in distillation
- Binding energy of the T_{bb}: $\sim 55\,\mathrm{MeV}$ (lower bound)
  $\rightarrow$ Consistent with other RHQ results
- BB^* scattering near threshold:
  - s-wave Lüscher analysis (good fit quality)
  - Found a shallow **virtual bound state** $2\,\mathrm{MeV}$ below threshold

Conclusion

- Investigation of BB^* system with RHQ action:
  - $m_\pi \approx 420$ MeV
  - Large basis of local and bilocal operators in distillation
- Binding energy of the T_{bb}: $\sim 55\ \mathrm{MeV}$ (lower bound)

  $\rightarrow$ Consistent with other RHQ results
- BB^* scattering near threshold:
  - s-wave Lüscher analysis (good fit quality)
  - Found a shallow **virtual bound state** $2\ \mathrm{MeV}$ below threshold
- Future plans:

Conclusion

- Investigation of BB^* system with RHQ action:
  - $m_\pi \approx 420$ MeV
  - Large basis of local and bilocal operators in distillation
- Binding energy of the T_{bb}: $\sim 55\,\mathrm{MeV}$ (lower bound)
  $\rightarrow$ Consistent with other RHQ results
- BB^* scattering near threshold:
  - s-wave Lüscher analysis (good fit quality)
  - Found a shallow **virtual bound state** $2\,\mathrm{MeV}$ below threshold
- Future plans:
  - Improve $B^{(*)}$-meson and tetraquark operators $\rightarrow$ More trustworthy spectrum

Conclusion

- Investigation of BB^* system with RHQ action:
  - $m_\pi \approx 420$ MeV
  - Large basis of local and bilocal operators in distillation
- Binding energy of the T_{bb}: $\sim 55\,\mathrm{MeV}$ (lower bound)
  $\rightarrow$ Consistent with other RHQ results
- BB^* scattering near threshold:
  - s-wave Lüscher analysis (good fit quality)
  - Found a shallow **virtual bound state** $2\,\mathrm{MeV}$ below threshold
- Future plans:
  - Improve $B^{(*)}$-meson and tetraquark operators $\rightarrow$ More trustworthy spectrum
  - Improve finite volume analysis (multiple channels, LHC)

Conclusion

- Investigation of BB^* system with RHQ action:
  - $m_\pi \approx 420$ MeV
  - Large basis of local and bilocal operators in distillation
- Binding energy of the T_{bb}: $\sim 55\,\mathrm{MeV}$ (lower bound)
  $\rightarrow$ Consistent with other RHQ results
- BB^* scattering near threshold:
  - s-wave Lüscher analysis (good fit quality)
  - Found a shallow **virtual bound state** $2\,\mathrm{MeV}$ below threshold
- Future plans:
  - Improve $B^{(*)}$-meson and tetraquark operators $\rightarrow$ More trustworthy spectrum
  - Improve finite volume analysis (multiple channels, LHC)
  - Multiple lattice spacings/volumes

Conclusion

- Investigation of BB^* system with RHQ action:
  - $m_\pi \approx 420$ MeV
  - Large basis of local and bilocal operators in distillation
- Binding energy of the T_{bb}: $\sim 55\,\mathrm{MeV}$ (lower bound)
  $\rightarrow$ Consistent with other RHQ results
- BB^* scattering near threshold:
  - s-wave Lüscher analysis (good fit quality)
  - Found a shallow **virtual bound state** $2\,\mathrm{MeV}$ below threshold
- Future plans:
  - Improve $B^{(*)}$-meson and tetraquark operators $\rightarrow$ More trustworthy spectrum
  - Improve finite volume analysis (multiple channels, LHC)
  - Multiple lattice spacings/volumes

Thank you for your attention!

References

References

- Leskovec, Luka et al. (2019). **"Lattice QCD investigation of a doubly-bottom $\bar{b}\bar{b}ud$ tetraquark with quantum numbers $I(J^P) = 0(1^+)$".** In: *Phys. Rev. D* 100.1, p. 014503. DOI: 10.1103/PhysRevD.100.014503. arXiv: 1904.04197 [hep-lat].
- Alexandrou, Constantia et al. (2024). **"$\overline{bb}ud$ and $\overline{bb}us$ tetraquarks from lattice QCD using symmetric correlation matrices with both local and scattering interpolating operators".** In: *Phys. Rev. D* 110.5, p. 054510. DOI: 10.1103/PhysRevD.110.054510. arXiv: 2404.03588 [hep-lat].
- Hoffmann, Jakob and Stefan Meinel (2026). **"Binding energy of the T_{bb} tetraquark from lattice QCD with relativistic and nonrelativistic heavy-quark actions".** In: *Phys. Rev. D* 113.11, p. 114516. DOI: 10.1103/j29k-6rx5. arXiv: 2603.12418 [hep-lat].
- Aoki, Sinya, Yoshinobu Kuramashi, and Shin-ichi Tominaga (2003). **"Relativistic heavy quarks on the lattice".** In: *Prog. Theor. Phys.* 109, pp. 383–413. DOI: 10.1143/PTP.109.383. arXiv: hep-lat/0107009.
- Hudspith, R. J. and D. Mohler (2022). **"Fully nonperturbative charm-quark tuning using machine learning".** In: *Phys. Rev. D* 106.3, p. 034508. DOI: 10.1103/PhysRevD.106.034508. arXiv: 2112.01997 [hep-lat].

References

AS, Andres and Jeremy R. Green (2026). **"Position-space sampling for local multiquark operators in lattice QCD using distillation and the importance of tetraquark operators for $T_{cc}(3875)^+$".** In: *Phys. Rev. D* 113.3, p. 034513. DOI: 10.1103/khhk-qw9n. arXiv: 2510.26459 [hep-lat].

Vujmilovic, Ivan et al. (2026). **"Electromagnetic Form Factors and Structure of the T_{bb} Tetraquark from Lattice QCD".** In: *Phys. Rev. Lett.* 136.16, p. 161901. DOI: 10.1103/jnsy-5nhj. arXiv: 2510.17549 [hep-lat].

Whyte, Travis, David J. Wilson, and Christopher E. Thomas (2025). **"Near-threshold states in coupled $DD^* - D^*D^*$ scattering from lattice QCD".** In: *Phys. Rev. D* 111.3, p. 034511. DOI: 10.1103/PhysRevD.111.034511. arXiv: 2405.15741 [hep-lat].

Backup slides

B and B^* effective energies

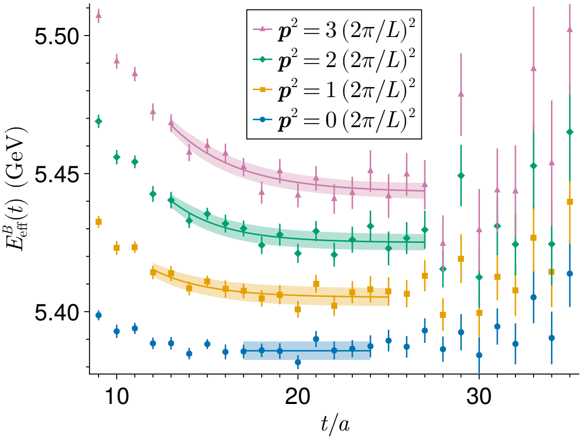

Figure: Effective energy E^B_{eff} of the B meson on N202 for the four lowest momenta.

T_{bb} dispersion relation

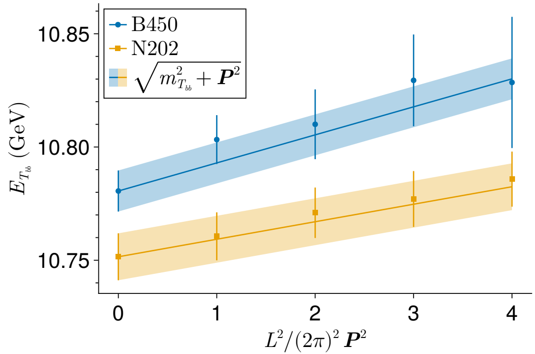

Figure: Ground-state energy vs. the integer total momentum squared. The curves show the continuum relation $E^2 = m_{T_{bb}}^2 + \boldsymbol{P}^2$ evaluated at the respective lattice masses.

Comparison of the two fitting strategies

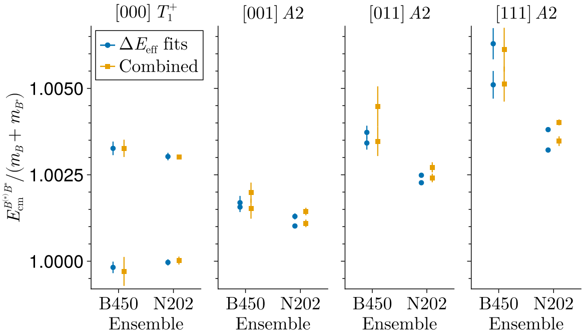

Figure: Excited finite-volume $B^{(*)}B^*$ energies from both fitting strategies and both ensembles, converted to the c.m. frame and normalized by the threshold energy $m_B + m_{B^*}$.

CLS gauge ensembles and RHQ parameters

Ensemble	$N_s^3 \times N_t$	β	a [fm]	$\kappa_u = \kappa_d = \kappa_s$	N_{cfg}	N_{src}	N_v	N_{sep}
B450	$32^3 \times 64$	3.46	0.0749	0.136890	1612	8	32	8
N202	$48^3 \times 128$	3.55	0.0633	0.137000	899	8	68	8

Ensemble	κ_b	ν	r_s	c_E	c_B
B450	0.054727	2.167	1.981	1.947	2.135
N202	0.068125	1.784	1.631	1.845	1.932

- $N_f = 3$ Wilson clover fermions
- $SU(3)$-flavour-symmetric point with physical $\frac{1}{3}(m_u + m_d + m_s)$
- $m_\pi \approx$ 420 MeV
- RHQ action for the b quark, tuned to 5 bottomonium masses and $c^2 = 1$